International Journal of Intelligent Networks 1 (2020) 148–156

Contents lists available at ScienceDirect

International Journal of Intelligent Networks

journal homepage: www.keaipublishing.com/en/journals/international-journal-of-intelligent-networks

# Deep Biomedical Image Classification Using Diagonal Bilinear Interpolation and residual network

Meghan Bani Assad *, Ronald Kiczales

*Faculty of Science, Computer Science, Vancouver Campus, The University of British Columbia, Vancouver, BC, Canada*

ARTICLE INFO

*Keywords:*
Diagonal
Bilinear
Interpolated
Deep residual network
Biomedical image classification

ABSTRACT

Considering the initiation of the biomedical emergent method, the amount of stockpiled and encapsulated biomedical pictures is swiftly growing each day in dispensaries, biomedical establishments, and laboratories. Hence, there is a need for a novel biomedical pictorial evaluation method to attain the necessities of the medical classification and diagnosis for various forms of disease utilizing biomedical images. Nonetheless, the current biomedical image categorization methods and approaches, including the global non-biomedical image categorization frameworks, cannot be replied to extract more novel image characteristics with unbalanced features. In this paper, we propose a novel deep feature extraction and classification method for biomedical images, called, Diagonal Bilinear Interpolated Deep Residual Network (DBI-DRSN). The DBI-DRSN method combines a balance of data or features via the Diagonal Bilinear Interpolation preprocessing model and classifies the features via fine-tuning through the Deep Residual Network model. In the research, it is concluded that the Diagonal Bilinear Interpolation delivered an in-depth computationally efficient feature, that could maintain the aspect ratio of the image in a significant manner, while the deep network could convey more robust and fine-tuned information used to classify the images. A detailed comparison of our method with conventional deep learning methods uses the public biomedical images and datasets evaluation of our projected approach for the classification of biomedical images.

## 1. Introduction

The Biomedical images are widely used in applications ranging from disease diagnosis, analyzing healthcare, validating pharmaceutical products, and so on. By divulging objects and areas other than the revolutionary aspect of common open eyes, biomedical images such as the microscopy can potentially bestow a significant feature that forms the novel objects. The arrangement of the Retinal Optical Coherence Tomography (OCT) images in an automatic and precise manner is considered to be highly essential to aid the ophthalmologist in macular disease diagnosis and grading accordingly. The conventional type of diagnosis and grading consists of identifying the size, number of macular lesions.

An innovative Lesion Aware Convolutional Neural Network (LACNN) technique was proposed in [1] for precise and accurate OCT retinal image classification. First, the Lesion Detection Network (LDN) was formulated to provide a considerable responsiveness map from a whole OCT viewpoint. The soft attention map was included in the categorization segment for the main aim of the weighted contribution of the localized convolution representation, therefore minimizing the computational time. Despite minimal computational time required for diagnosis and grading of retinal OCT images, with unbalanced data, accuracy is said to be compromised. To address this issue in this work, image augmenting is addressed via the Diagonal Bilinear Interpolation preprocessing model by significantly increasing the diversity of data (i.e., pixels) without actually collecting new data (i.e., new pixels).

The Convolutional Neural Network (CNN) method linked up with Graph Cut (GC) optimization, called CNN-GC, was proposed in [2] with the objective of automatic classification of biomedical, i.e., CT chest images. The algorithm used in CNN-GC applied three different steps, namely, scale-space particle segmentation, a 3D convolutional neural network and graph cuts optimization. The scale-space particle segmentation was initially applied to the input images to isolate the vessels in an efficient manner.

Next, the three-dimensional convolutional neural network (CNN) was functional to isolate the vessels with the purpose of obtaining the initial categorization of vessels, considering the GC optimization that is applied in the classification of results, which is useful for finding the refined results. Despite accuracy and computational efficiency achieved for

* Corresponding author.
*E-mail addresses:* meghanabani@hotmail.com (M.B. Assad), ronaldkiczales@outlookmail.com (R. Kiczales).

https://doi.org/10.1016/j.ijin.2020.11.001
Received 2 October 2020; Received in revised form 15 November 2020; Accepted 21 November 2020

biomedical image classification, with large-scale collected biomedical images,the time and accuracy will be compromised. To address this issue, fine-tune classification is achieved via a residual network, therefore contributing both accuracy and computational efficiency even for a large-scale collected deep neural network for biomedical retinal OCT images.

Inspired by this as well as the relation between bilinear interpolation and fine-tuning training via a deep network, this paper proposes a Diagonal Bilinear Interpolated Deep Residual Network (DBI-DRSN) method for biomedical image classification with higher accuracy. The rational contribution has been summed as;

- In relation to the unbalanced information that is not in contrast to the grading of retinal OCT parts and large-scale biomedical images of different types harder to classify, we imitate the Bilinear Interpolation, specifically motivated by the interpolation theory and the training works. These enable the extraction of more computational efficacy and robust data that promise massive improvement in the biomedical image categorization.
- Bilinear Interpolation is initially applied in the image categorization issues, in this research, which preprocesses the OCT retinal images provided as input that enhance complete utility of information and content features according to the interpolation function instead of the time-related lesion aware method followed in the prevailing issues, assisting the retinal OCT data being preprocessing in a computationally efficient manner.
- A Deep Residual Convolute Classification algorithm is recommended in this research considering the residual activation function and spatial dimension. By applying these two features, the classification between retinal images is made better in relation to contemporary works.
- Performed experiments and critical comparison on retinal OCT images, validatingthe efficiency of the projected technique.

The remaining section of the research is planned as follows. To begin with, a background evaluation is given in Section 2. After that, a proposed methodology is given in section 3. Subsequently, the experimental findings are given to indicate the efficiency of the recommended method in section 4. A detailed discussion along with the tabular and graphical representation is given in Section 5. Lastly, this research is ended in Section 6.

## 2. Related works

Damage of DNA in recent years is considered as vital research in the biomedical and medical fields. Several internal and external aspects of human cells are said to be influenced to get damage unintentionally. For effective classification, images belonging to four classes were trained using a convolutional neural network [3], therefore contributing to accuracy. A critical appraisal of deep learning-based image segmentation, their achievements and challenges were detailed in [4]. However, with similar defects found difficulty in classifying, accurate classification was not said to be achieved. To address this issue, pictorial long-term and short-term memory-centered integration frameworks were designed in [5] to not only address precise classification but also address the overfitting problem involved during classification. This was achieved via Stack Convolutional Auto Encoders (SCAE). An analysis to classify and biomedical retrieval images were presented in [6].

Machine Learning (ML) has spackled a fundamental interest over the past few years, mostly in the field of deep learning, which involved the bifurcate of ML using the multiple layer neural network. Deep learning has progressed remarkably well in the analysis and classification of images, mostly because of the application of the convolutional neural networks (CNN).

In [7], deep learning was applied in medical imaging. However, with smaller training data set, CNN was not found to be widely accepted. In [8], deep learning was combined with handcrafted visual features, therefore contributing to medical image classification accuracy. Despite improvement observed in classification accuracy, with the absence of prior knowledge, the prediction was not made in an efficient manner. To address this issue, Anatomically Constrained Neural Networks (ACNN) was designed in [9] via a learnt nonlinear representation of the shape on the multimodal cardiac dataset.

Skeletal muscles of males and females possess definite differentiations concerning metabolism, composition, strength, endurance while performing classification. A deep learning-based mechanism to differentiate between males and females based on the skeletal muscles via saliency and occlusion maps was presented in [10]. However, the convergence rate was not found to be optimal. A Multi-scale Convolutional Mixture of Expert (MCME) ensemble method was proposed in [11] by utilizing a correlated multivariate component for each model, therefore contributing, precision rate via independent Gaussian components. Different color normalization techniques were applied in [12] for classification between benign and malignant cases.

In [13], a novel Hybrid recurrent and convolutional deep neural network is vital for the categorization of the Breast Cancer. In reference to the multiple level characteristic representations of the histopathological pictorial patch, the technique incorporated the merits of a recurrent and convolutional neural network, therefore preserving the spatial correlations between images. Yet another deep learning in medical image processing including prior knowledge regarding processing was presented in [14]. An overview of deep learning concentrating on MRI medical images was investigated in [15].

Though several biomedical image classification methods were designed, minor variations between the various forms of ailments and similar images from one class were never captured. A critical convolutional neural network was obtained in [16] hence integrating a minor layer feature composed of a deep layer feature. Furthermore, it was analyzed that detailed local features were provided via shallow layers, and high-level information was obtained via deep layers. Yet another confidence score based classification rule was designed in [17] using the subspace analysis technique contributing to a higher level of classification accuracy.

To perform hyperspectral image classification, a novel iterative linearly constrained minimum variation category framework was designed in [18] for the classification of brain tissue. However, the above-said process was found to be time-consuming. To minimize the time being consumed, a drop out based strategy was adopted in [19] to classify between endoscopic and endomicroscopy images. Supervised machine learning technique based on priority for retinal OCT imaging data was presented in [20].

The above Deep Biomedical Image Classification methods and algorithms discussed above had certain issues in that they either adopted convolution neural networks or directly applied conventional method for biomedical image classification. In conventional methods, regardless of the features used, without applying any preprocessing model separately, it takes computationally larger time to categorize the pictures. Moreover, a considerable segment of literature about the medical image classification provided above, without fine-tuning the features, robust classification of biomedical images are not said to be obtained, therefore compromising the rate of accuracy. In practice, we usually need to perform a separate preprocessing and classification task. To solve these issues and improve the performance of biomedical image classification, we present our new method, Diagonal Bilinear Interpolated Deep Residual Network (DBI-DRSN) in the following sections.

## 3. Methodology

This part provides an in-depth evaluation of the methods used to compose this research. To start with, a preprocessing model based on Diagonal Bilinear Interpolation is first presented to obtain computationally efficient preprocessed features by balancing the features based on horizontal, vertical and diagonal proportionality. In this way,

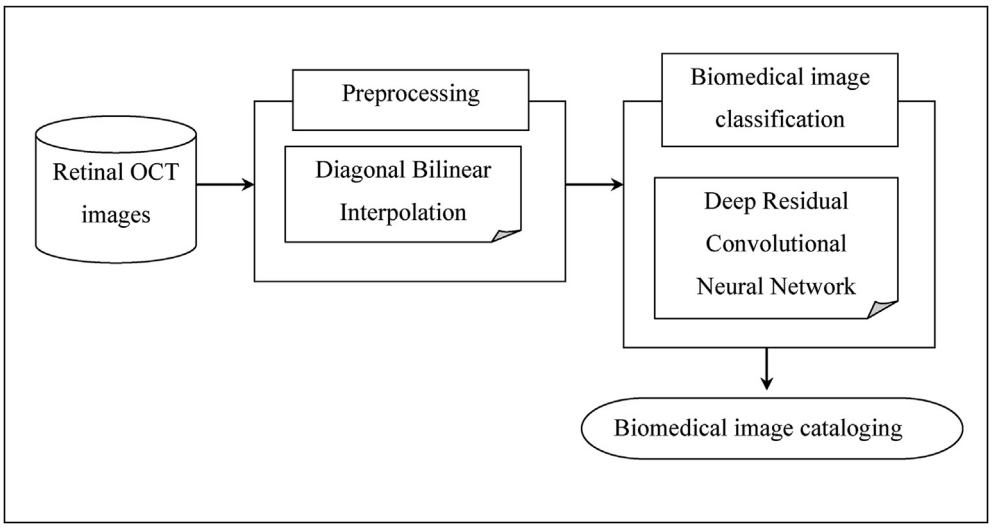


**Fig. 1.** Block diagram of the Diagonal Bilinear Interpolated Deep Residual Network.

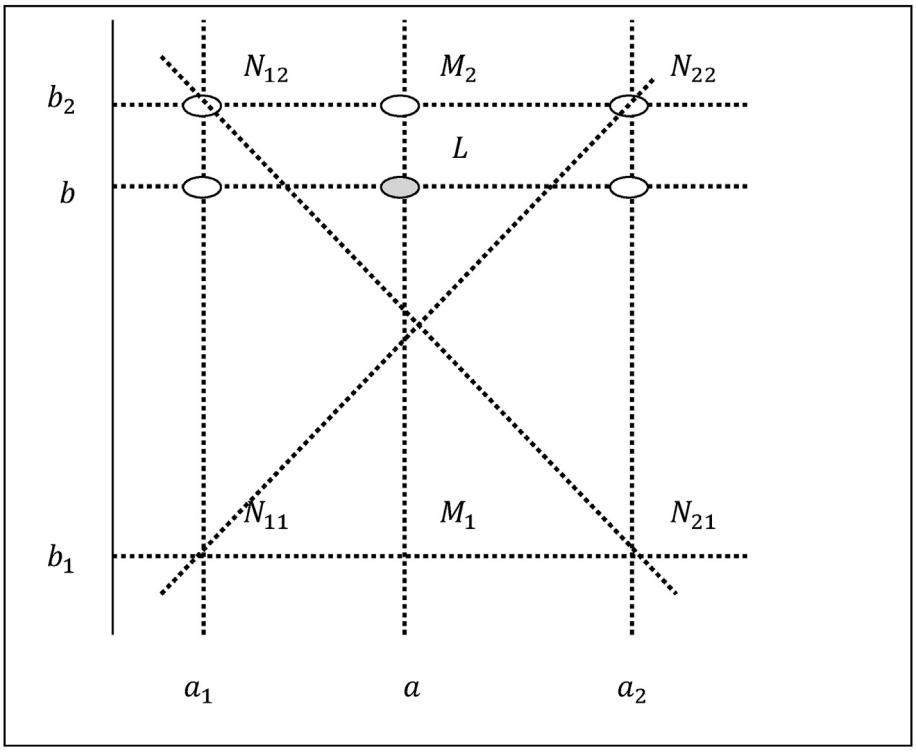


**Fig. 2.** Sample diagonal bilinear interpolation.

computationally efficient feature with image augmenting is said to be attained, therefore laying a platform for efficient biomedical image classification. Then a fine-tuned Deep Residual Network for Biomedical Image Classification is presented for more discriminative and robust representations. The flowchart of the whole framework, Diagonal Bilinear Interpolated Deep Residual Network for biomedical image classification, is illustrated in Fig. 1.

In reference to the image presented above, the projected technique, Diagonal Bilinear Interpolated Deep Residual Network (DBI-DRN) for biomedical image classification, includes two steps. The first step involves preprocessing using the Diagonal Bilinear Interpolation model. With this preprocessing model, computationally efficient features for classification are obtained. Next, step performs the actual classification using the Deep Residual Convolutional Neural Network model. With this classification model, significant classification is said to be attained. The elaborate description of the proposed method is explained below.

### 3.1. Diagonal bilinear interpolation preprocessing

Since there is a huge variation in image resolutions of the retinal OCT images, ranging from the large scale to the smallest scale, resizing and cropping these retinal OCT images into required size results in either distortion or information loss, in this study, we resize these images to a uniform scale while maintaining the aspect ratio, by applying a Diagonal Bilinear Interpolation (DBI) Preprocessing model.The figure shows the sample DBI preprocessing model followed for biomedical retinal OCT image classification.

As depicted in the above figure, the Diagonal Bilinear Interpolation

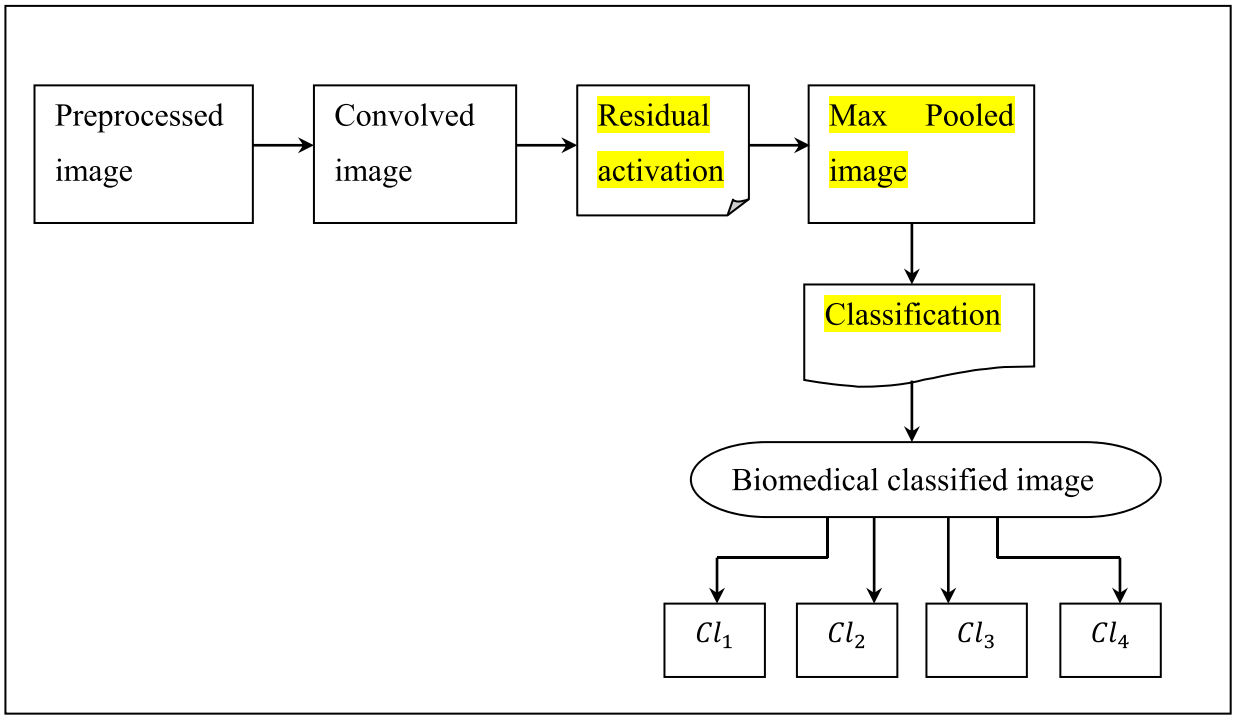


**Fig. 3.** Block diagram of Deep Residual Convolutional Neural Network.

model is followed as a preprocessing step with the purpose of interpolating images (i.e.,functions) of two variables (i.e., between two pixels '$a$' and '$b$'). The Diagonal Bilinear Interpolation is performed using linear interpolation first in one direction (i.e., horizontal), and then again in the other direction (i.e., vertical) and finally in the third direction (i.e., diagonal).

Though linearity is said to be followed in each step during the preprocessing of retinal OCT images provided as input in the sampled values and in the position, the interpolation as an entire process is not said to be linear but instead orthogonal in the sample image. The pseudo-code representation of Diagonal Bilinear Interpolated Preprocessing is given below.

**Algorithm 1**. Diagonal Bilinear Interpolated Preprocessing

| |
|---|
| **Input**: Images '$I = I_1, I_2, \ldots, I_n$' |
| **Output**: Computationally efficient preprocessed images '$PI$' |
| 1: **Initialize**'$PI$' at points '$N_{11} = (a_1, b_1)$', '$N_{12} = (a_1, b_2)$', '$N_{21} = (a_2, b_1)$' , '$N_{22} = (a_2, b_2)$' |
| 2: **Begin** |
| 3: **For** each input OCT Images '$I$' |
| 4: Perform linear interpolation in the horizontal direction using (1) and (2) |
| 5: Perform linear interpolation in the vertical direction using (3), (4) and (5) |
| 6: Perform linear interpolation diagonally using (6) |
| 7: **Return** (Preprocessed images) |
| 8: **End for** |
| 9: **End** |

As given in the above Diagonal Bilinear Interpolated Preprocessing algorithm, for each retinal OCT images obtained as input, the objective remains in preprocessing the raw input image in a computationally efficient manner, therefore providing a mechanism for accurate and precise biomedical image classification. The preprocessing applied in our work mainly concentrates on image normalization.

Each original retinal OCT image is normalized along its horizontal, vertical, and diagonal direction resulting along with its shortest side into a preprocessing image while maintaining the aspect ratio of the image.

Let us consider that if we want to identify the preprocessed image value '$PI$' at the point '$a,b$' with the basic assumption that the pixel value of '$PI$' at the four points '$N_{11} = (a_1,b_1)$', '$N_{12} = (a_1,b_2)$', '$N_{21} = (a_2,b_1)$' and '$N_{22} = (a_2,b_2)$' respectively. Then, linear interpolation is first done in the '$a$' direction. This is expressed as given below.

$$PI(a,b_1) = \frac{a_2 - a}{a_2 - a_1} PI(N_{11}) + \frac{a - a_1}{a_2 - a_1} PI(N_{21}) \quad (1)$$

$$PI(a,b_2) = \frac{a_2 - a}{a_2 - a_1} PI(N_{12}) + \frac{a - a_1}{a_2 - a_1} PI(N_{22}) \quad (2)$$

Then, linear interpolation is next done in the '$b$' direction.

$$PI(a,b) = \frac{b_2 - b}{b_2 - b_1} * PI(a,b_1) + \frac{b - b_1}{b_2 - b_1} * PI(a,b_2) \tag{3}$$

$$= \frac{b_2 - b}{b_2 - b_1} * \left[\frac{a_2 - a}{a_2 - a_1} PI(N_{11}) + \frac{a - a_1}{a_2 - a_1} PI(N_{21})\right] + \frac{b - b_1}{b_2 - b_1} * \left[\frac{a_2 - a}{a_2 - a_1} PI(N_{12}) + \frac{a - a_1}{a_2 - a_1} PI(N_{22})\right] \tag{4}$$

$$= \frac{1}{(a_2 - a_1)(b_2 - b_1)} [a_2 - a\ a - a_1] \begin{bmatrix} PI(N_{11})PI(N_{12}) \\ PI(N_{21})PI(N_{22}) \end{bmatrix} \tag{5}$$

Finally, the linear interpolation is performed diagonally, as given below.

$$PI(b_1,b_2) = \frac{(N_{22} - N_{11})(N_{12} - N_{21})}{(a_2 - a_1)(b_2 - b_1)} \tag{6}$$

### 3.2. Deep Residual Convolutional Neural Network

When training the biomedical images for classification, the preprocessed images are acquired as input (see Fig. 2).

Convolution Neural Network comprises of multiple processing layers that learn a different abstract representation of levels. By integrating the layers present via the Deep Residual factor in CNN preserves the discriminative and robust features. The CNN comprises of a series of convolutional layers and pooling layers. Fig. 3 shows the block diagram of the Deep Residual Convolutional Neural Network model.

As depicted in the above figure, the CNN in the proposed work is called as Deep Residual CNN because of the application of residual activation as the activation function that preserves the discriminative and robust features and accordingly classifies the biomedical images in a significant manner. The pseudo-code representation of Deep Residual Convolute Classification is given below.

**Algorithm 2.** Deep Residual Convolute Classification algorithm

| |
|---|
| **Input**: preprocessed images '*PI*' |
| **Output**: Robust classification of images |
| 1: **Begin** |
| 2: **For** each preprocessed images '*PI*' |
| 3: Perform feature extraction by convolving preprocessed image using (7) |
| 4: Evaluate residual activation function using (8) and (9) |
| 5: Reduce the spatial dimension by pooling the convolved image using (10) |
| 6: Perform classification using (11) |
| 7: **Return** (classified images) |
| 8: **End for** |
| 9: **End** |

As given in the above algorithm, to start with, the preprocessed image given as input, the convolution operation is performed with the objective of extracting the features required for further classification. This is performed with the objective of preserving the relationship between pixels by learning the biomedical image features via small squares. This is mathematically expressed as given below.

$$b_j^l = fun\left(B_j^l + \sum W_{i,j}^{l-1} * a_i^l\right) \tag{7}$$

From the above equation (7), '*l*' corresponds to the '*lth*' layer for extracting relevant features and '*fun*' refers to the activation function and. '$a_i$' and '$b_j$' refers to the '*ith*' input feature map and '*jth*' output feature map, while. '$w_{i,j}$' represents the convolution kernel between. '$a_i$' and '$b_j$', '$B_j$' referring to the bias and '*' is the convolution operation respectively. For faster convergence,the residual activation function is used in this work and is expressed as given below.

$$fun\ (a_i) = b_j - Relu[a_i] \tag{8}$$

$$fun\ (a_i) = b_j - Relu\ [\varphi(a_i)] \tag{9}$$

From the above equation (8), '$a_i$' and '$b_j$' represent the input and output of the corresponding '*lth*' layer feature map with '*Relu* ()' corresponding to the rectified linear unit and '*fun*()' representing the residual activation function, respectively. Besides, dimension matching is performed via equation (9) via linear estimation '$\varphi$' and corresponding dimensional matching is said to be achieved.

Followed by the convolving of preprocessed images, the next step remains in continuously minimizing the spatial dimensions of the extracted features to minimize the parameter estimation via max pooling. The pooling in our work is performed via max-pooling with a '3*3' window and is expressed as given below.

$$b_{j,l}^j = MAX\left(a_{j,3,l3}^i\right) \tag{10}$$

From the above equation (10), each element or pixel incorporated in the output element map. '$b_j$' is pooling from the '3*3' overlapping part in the input element map. '$a_j$' respectively. Finally, a softmax layer is connected to the spatial dimension reduced features to predict '$z$' different classes via probability factor, and the feature will rasterize into '$a$,' corresponding to a column feature vector.

$$Prob(b = j|a,\theta) = \frac{e^{\theta_j^T a}}{\sum_{j=1}^{z} e^{\theta_j^T a}} \tag{11}$$

From the above equation (11) the target contains '$z$' different classes (i.e., four different classes, '$Cl_1$ = *CNV*', '$Cl_2$ = *DME*', '$Cl_3$ = *DRUSEN*'' and. '$Cl_4$ = *NORMAL*' for retinal OCT images).

## 4. Experimental setup

To effectively evaluate the performance of the recommended model, the DBI-DRSN technique is implemented in MATLAB simulator. This simulation process of the DBI-DRSN method considered Retinal OCT images extracted from https://www.kaggle.com/paultimothymooney/kermany2018#NORMAL-1038998-1.jpeg. The simulation of the DBI-DRSN method is performed for varying numbers of images, considering different types of images considered as input, i.e., DME, Normal, DRUSEN and CNV.

The retinal OCT imageriesencompass four different types of images that capture high-resolution cross-sections of the retinas of living patients observed from 242 four different types of inputs. The simulation performance of the DBI-DRSN method is measured in terms of

**Table 1**
Tabulation for communication time.

| Number of retinal images | Communication time (ms) | | |
|---|---|---|---|
| | DBI-DRSN | LACNN | CNN-GC |
| 15 | 0.375 | 0.675 | 0.9 |
| 30 | 0.535 | 0.815 | 1.135 |
| 45 | 0.715 | 0.925 | 1.145 |
| 60 | 0.925 | 0.955 | 1.535 |
| 75 | 1.025 | 1.135 | 1.615 |
| 90 | 1.135 | 1.245 | 1.725 |
| 105 | 1.455 | 1.535 | 1.935 |
| 120 | 1.625 | 1.685 | 1.985 |
| 135 | 1.835 | 1.915 | 2.035 |
| 150 | 1.945 | 2.035 | 2.135 |

communication overhead, communication time and classification accuracy. The simulation result of the DBI-DRSN methodis compared with two existing methods namely LACNN [1] and CNN-GC [2].

## 5. Discussion

The simulation result of the DBI-DRSN method is discussed in this section. The performance result of the proposed DBI-DRSN method is compared with two conventional works namely LACNN [1] and CNN-GC [2] using metrics such as communication overhead, communication time and classification accuracy and analyzed with the help of tables and graphs.

### 5.1. The performance measure of communication time

Several modern imaging techniques, specifically biomedical images for healthcare systems, require the actions of multiple computations to be performed at much faster speed with minimum convergence rate. Hence, communication time is the most prevalent entity that biomedical image techniques require. Hence, the communication time is measured as the performance metric. The communication time, in other words, denotes the product of the overall amount of retinal pictures utilized in evaluating the duration of communication involved while performing preprocessing. It is expressed as given below.

$$CT = \sum_{i=1}^{n} I_i * Time\ [PP] \tag{12}$$

Based on the equation stated in (12), the time is taken for communication to take place '*CT*' is considered in reference to the overall number of retinal images $I_i$', used for simulation, including the duration taken for preprocessing *Time* [*PP*]. This is evaluated based on milliseconds (ms). The example of calculations used for communication duration based on the recommended DBI-DRSN and existing, LACNN [1] and CNN-GC [2] is represented as.

Sample calculation for communication time.

- **ProjectedDBI-DRSN**:This is in relation to '15' retinal image number considering the time-consumed and experimentation in pre-processing one retinal image as 0.025*ms*'; hence the general communication duration is considered as:

$$CT = 15*0.025ms = 0.375ms$$

- **Existing LACNN** [1]: This is in relation to '15' retinal image number considering the time-consumed and experimentation in pre-processing one retinal image as 0.045*ms*; hence the general communication duration is considered as:

$$CT = 15*0.045ms = 0.675ms$$

- **Existing CNN-GC** [2]: This is in relation to '15' retinal image number considering the time-consumed and experimentation in pre-processing one retinal image as 0.060*ms*'; hence the general communication duration is considered as:

$$CT = 15*0.060ms = 0.90ms$$

The first obtained results are presented in Table 1 where we show the communication time incurred while performing preprocessing by our proposed method, DBI-DRSN when it is compared with the existing LACNN [1] and CNN-GC [2] respectively.

Fig. 4, given above, depicts the communication time with respect to different numbers of retinal images obtained at different time intervals

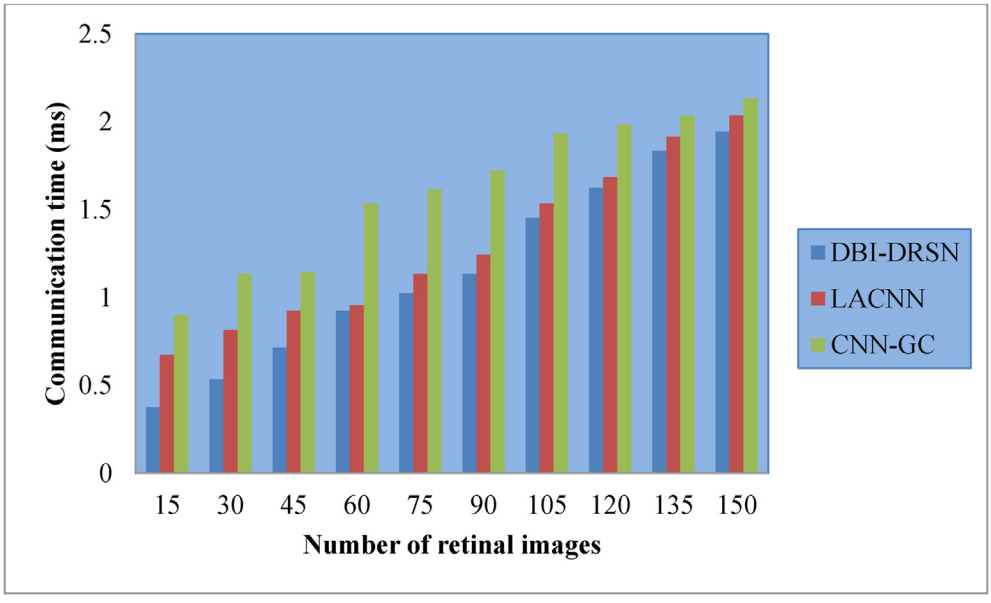


**Fig. 4.** Graphical representation of communication time.

**Table 2**
Tabulation for communication overhead.

| Number of retinal images | Communication overhead (KB) | | |
|---|---|---|---|
| | DBI-DRSN | LACNN | CNN-GC |
| 15 | 30 | 45 | 60 |
| 30 | 50 | 75 | 90 |
| 45 | 65 | 90 | 110 |
| 60 | 70 | 110 | 130 |
| 75 | 90 | 120 | 150 |
| 90 | 105 | 135 | 170 |
| 105 | 120 | 140 | 180 |
| 120 | 145 | 170 | 210 |
| 135 | 160 | 190 | 230 |
| 150 | 190 | 220 | 250 |

with different subjects. From the figure, it is evident that boosting the retinal image number enhances the image number considered for classification increases and hence the communication time during also preprocessing increases. Besides, the increase is not proportionality due to the presence of noise is certain images while the noise level was differing in certain other types of images. Due to this reason, the changes in communication time are also seen for a different number of retinal images.

However, based on the results of a simulation, it is considered that the communication time using the DBI-DRSN method is comparatively lesser than the existing LACNN [1] and CNN-GC [2]. This is because of the incorporation of Diagonal Bilinear Interpolation for the preprocessing of retinal images. When compared to the other interpolation, diagonal bilinear interpolation possess the advantage of obtaining the values of only the four nearest pixels located in the diagonal directions from a given pixel to identify the appropriate preprocessed values of that images. With this, the communication time for preprocessing using the DBI-DRSNtechnique is considerably diminished by approximately 24% in reference to [1] and about 38% different from [2] respectively.

### 5.2. The performance measure of communication overhead

As far as biomedical images are concerned, when operated through a deep network, a significant amount of memory is said to be consumed, either while storing or while retrieval via a network. Hence, one of the important parameters while analyzing medical data for biomedical image classification is communication overhead. The communication overhead, in other words, denotes the product retinal image number utilized for evaluating and the consumed memory during pre-processing. It is shown through the mathematical formula below.

$$CO = \sum_{i=1}^{n} I_i * MEM\,[PP] \tag{13}$$

Based on the equation shown above, the Communication Overhead '$CO$' is indicated considering the retinal image number used during experimentation.'$I_i$' and the memory expended during pre-processing '$MEM\,[PP]$'. It is measured in terms of kilobytes (KB). The sample calculation for communication overhead using the proposed DBI-DRSN and existing, LACNN [1] and CNN-GC [2] is given below.

Sample calculation for communication overhead.

- **Proposed DBI-DRSN**: With '15' number of retinal images considered for simulation and the memory consumed during pre-processing for single retinal image being '2$KB$', the overall communication overhead is measured as given below.

$$CO = 15*2KB = 30KB$$

- Existing LACNN [1]: With '9' number of retinal images considered for simulation and the memory consumed during pre-processing for single retinal image being '3$KB$', the overall communication overhead is measured as given below.

$$CO = 15*3KB = 45KB$$

- **Existing CNN-GC** [2]: With '9' number of instances considered for simulation and the memory consumed during pre-processing for single retinal image being '4$KB$', the overall communication overhead is measured as given below.

$$CO = 15*4KB = 60KB$$

The second obtained results are presented in Table 2 where we show the communication overhead while performing preprocessing by our proposed method, DBI-DRSN when it is compared with the existing LACNN [1] and CNN-GC [2] respectively.

Fig. 5, given above, depicts the communication overhead with respect to 150 different numbers of retinal images. Here, the x-axis refers to the

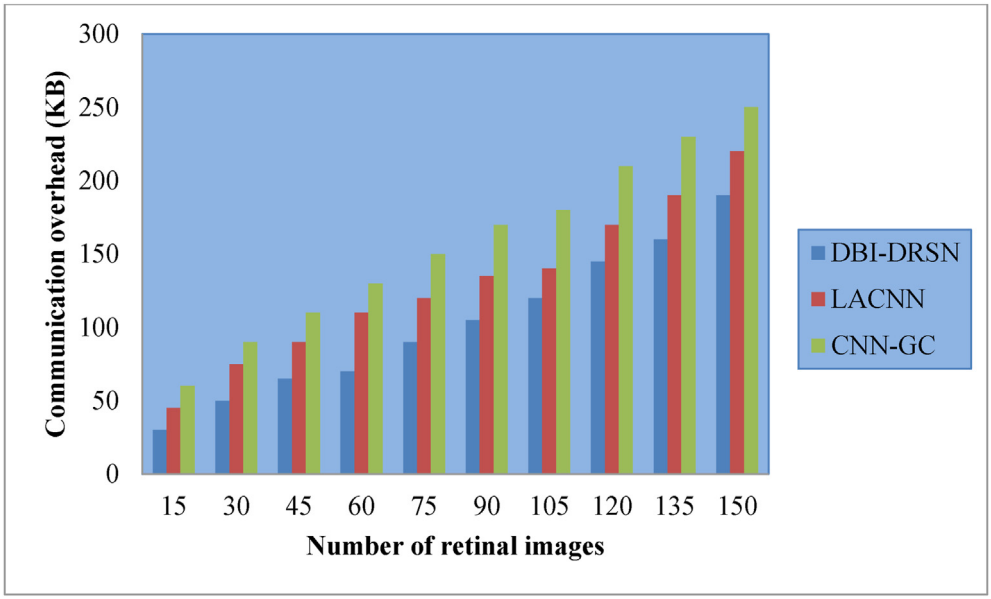


**Fig. 5.** Graphical representation of communication overhead.

**Table 3**
Tabulation of classification correctness.

| Number of retinal images | Classification accuracy (%) | | |
|---|---|---|---|
| | DBI-DRSN | LACNN | CNN-GC |
| 15 | 93.33 | 86.66 | 80 |
| 30 | 92.25 | 85.35 | 78.35 |
| 45 | 91.45 | 84.15 | 77.15 |
| 60 | 90 | 82.35 | 75.35 |
| 75 | 89.35 | 80.15 | 74.35 |
| 90 | 91.24 | 81.35 | 75.85 |
| 105 | 92.35 | 82.45 | 77.25 |
| 120 | 93.15 | 84.35 | 79.35 |
| 135 | 92.25 | 82.15 | 72.45 |
| 150 | 90.45 | 83.25 | 70.35 |

number of images gathered during various moments considering the varied number of individuals and the y-axis denoting communication overhead measured in terms of kilobytes (KB). From the above Fig. 5, it is inferred that the number of retinal images is directly proportional to the communication overhead. In other words, with the increase in the number of retinal images, the size of the retinal images increases and therefore the communication overhead incurred during preprocessing also increases.

However, from the sample calculations provided above as the simulation, the communication overhead incurred by the DBI-DRSN method is comparatively lesser than the existing LACNN [1] and CNN-GC [2] methods, respectively. This is because of the application of the Diagonal Bilinear Interpolated Preprocessing algorithm. By applying this algorithm, preprocessing is only concentrated towards image normalization, where the original retinal OCT image given as input is normalized along with its three directions, horizontal, vertical and diagonal direction while maintaining the aspect ratio of the image. With this, the preprocessing of images is taken place at a higher convergence rate and therefore reducing the communication overhead using the DBI-DRSN technique by 14% contrasted to [1], including 32% different from [2] respectively.

### 5.3. The performance measure of classification accuracy

Finally, the parameter required to analyze biomedical images is the classification accuracy rate. Higher the rate of classification accuracy, better is the proposed method and vice versa. In other words, classification accuracy '*CA*' refers to the percentage ratio of the retinal image number categorically grouped $I_i(CC)$' based on the overall amount of retinal images. '$I_i$' in relation to the experiments done. This is evaluated based on a percentage (%) and expressed as given below.

$$CA = \sum_{i=1}^{n} \frac{I_i(CC)}{I_i} * 100 \tag{14}$$

The sample calculation for categorization competency [14] based on the projected DBI-DRSN and the present, LACNN [1] and CNN-GC [2] indicated below.

Sample calculation for classification accuracy.

- **Proposed DBI-DRSN**:In reference to '15' retinal image number useful for experimentation, and '14' retinal images that have been categorized correctly, the general categorization efficacy rate is considered as;

$$CA = \frac{14}{15} * 100 = 93.33\%$$

- **Existing LACNN** [1]: In reference to '13' retinal image number useful for experimentation, and '14' retinal images that have been categorized correctly, the general categorization efficacy rate is considered as;

$$CA = \frac{13}{15} * 100 = 86.66\%$$

- **Existing CNN-GC** [2]: In reference to '12' retinal image number useful for experimentation, and '14' retinal images that have been categorized correctly, the general categorization efficacy rate is considered as;

$$CA = \frac{12}{15} * 100 = 80\%$$

Finally, the classification accuracy results are shown in Table 3, where the categorization correctness measures the number of retinal images correctly classified using the proposed method, GFB-CNN, existing Adaptive IoT enabled CPS [1] and IoMT-PLM [2] respectively.

Fig. 6 above shows the classification accuracy with respect to 150 different numbers of retinal images, ranging between four different types of images, '*CNV*,' Choroidal Neo Vascularization, '*DME*,' Diabetic Maular

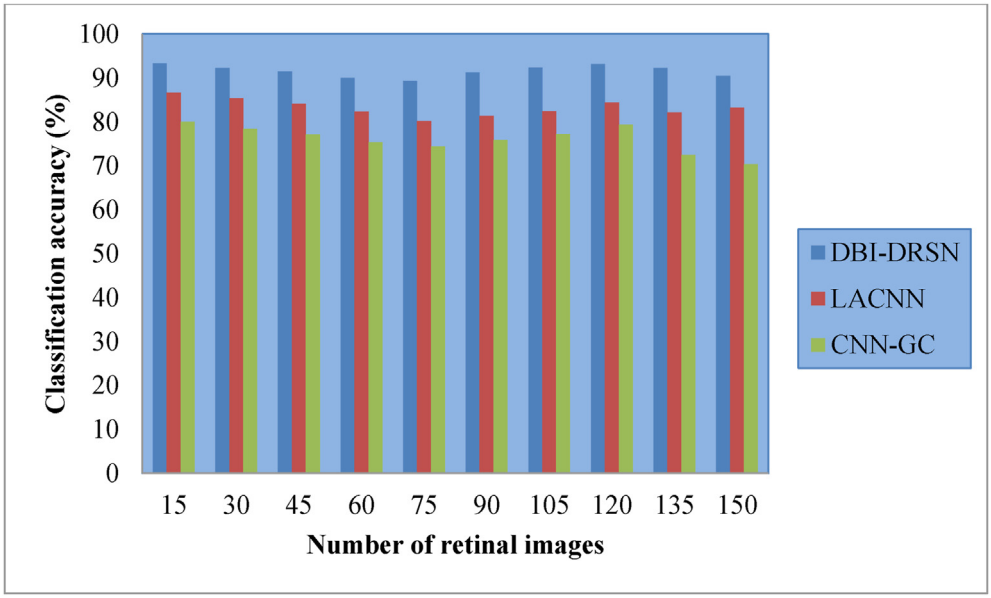


**Fig. 6.** Graphical representation of classification accuracy.

Edema, '*DRUSEN*,' and '*NORMAL*' respectively. With the x-axis representing the number of retinal images provided as input, the y-axis observes the classification accuracy using three different methods. From the figure, it is inferred that the number of retinal images is neither directly proportional nor inversely proportional to the classification accuracy. This is because with four different types of retinal images considered for experimentation, the noise also differs accordingly.

However, the classification accuracy is found to be better using DBI-DRSN when compared to the existing LACNN [1] and CNN-GC [2] respectively. This is because of the application of the Deep Residual Convolute Classification algorithm. By applying this algorithm, the relationship between pixels is maintained via small squares. Besides, with the incorporation of residual activation function, the dimension matching between the retinal images are said to be made in a significant manner. Therefore, the categorization correctness based on the DBI-DRSN technique is located to be more effective by 10% contrasted to [1] and about 21% contrasted [2] correspondingly.

## 6. Conclusion

The Diagonal Bilinear Interpolated Deep Residual Network (DBI-DRSN) method used to classify the biomedical image is formulated with the purpose of advancing the categorization correctness rate of retinal OCT medical data analysis with minimum communication time and communication overhead. The objective of the DBI-DRSNmethod is attained with the application of the Deep Residual Convolute Classification algorithm. The proposed DBI-DRSNmethod increases the classification accuracy rate with the number of retinal images being correctly classified with minimal time by classifying the computationally efficient pre-processing feature for biomedical image classification as compared to existing works. Also, the proposed DBI-DRSN method reduces the time and overhead because of the application ofthe Diagonal Bilinear Interpolated Preprocessing algorithm achieving image normalization while maintaining the image aspect ratio when compared to conventional works. Furthermore, the proposed DBI-DRSNmethod increases the classification accuracy that learns different levels of abstraction by preserving the discriminative and robust features via Deep Residual Convolute Neural Network as contrasted with the contemporary works. The status of the proposed DBI-DRSNmethod is determined in terms of communication time, communication overhead and classification accuracy with respect to a different number of retinal images and compared with two conventional methods. The simulation result demonstrates that the proposed DBI-DRSNmethod gives better performance if contrasted to the conventional works.

## Declaration of competing interest

The authors declare that they have no known competing financial interests or personal relationships that could have appeared to influence the work reported in this paper.

## References

[1] Leyuan Fang, Chong Wang, Shutao Li, Hossein Rabbani, Xiangdong Chen, Zhimin Liu, Attention to lesion: lesion-aware convolutional neural network for retinal optical coherence Tomography image classification, IEEE Trans. Med. Imag. 38 (8) (Apr 2019) 1959–1970.

[2] Pietro Nardelli, Daniel Jimenez-Carretero, David Bermejo-Pelaez, George R. Washko, Farbod N. Rahaghi, Maria J. Ledesma-Carbayo, Raul san jose estepar, "pulmonary artery-vein classification in CT images using deep learning", IEEE Trans. Med. Imag. 37 (11) (Nov. 2018).

[3] Umit Atila, Yusuf Yargı Baydilli, Eftal Sehirli, Muhammed Kamil Turan, "Classification of Dna Damages on Segmented Comet Assay Images Using Convolutional Neural Network", Computer Methods and Programs in Biomedicine, Elsevier, Nov 2019.

[4] Mohammad Hesam Hesamian, Wenjing Jia, Xiangjian He, Paul Kennedy, Deep learning techniques for medical image segmentation: achievements and challenges, J. Digit. Imag. 32 (4) (May 2019) 582–596. Springer.

[5] Yudi Zhao, Kuangrong Hao, Haibo He, Xuesong Tang, Bing Wei, A Visual Long-Short-Term Memory Based Integrated CNN Model for Fabric Defect Image Classification, Elsevier, Neurocomputing, Oct 2019.

[6] Leila Cristina C. Bergamasco, Fátima L.S. Nunes, "Intelligent Retrieval and Classification in Three-Dimensional Biomedical Images — A Systematic Mapping", Computer Science Review, Elsevier, Oct 2018.

[7] Paras Lakhani, Daniel L. Gray, Carl R. Pett, Paul Nagy, George Shih, Hello world deep learning in medical imaging, J. Digit. Imag. 31 (3) (May 2018) 283–289. Springer.

[8] Jianpeng Zhang, Yong Xia, Yutong Xie, Michael Fulham, David Dagan Feng, Classification of medical images in the biomedical literature by jointly using deep and handcrafted visual features, IEEE Journal of Biomedical and Health Informatics 22 (5) (Sept. 2018).

[9] Ozan Oktay, Enzo Ferrante, Konstantinos Kamnitsas, Mattias Heinrich, Wenjia Bai, Jose Caballero, A. Stuart, Antonio de Marvao Cook, Timothy Dawes, Declan P. O'Regan, Bernhard Kainz, Ben Glocker, Daniel Rueckert, Anatomically constrained neural networks (ACNNs): application to cardiac image enhancement and segmentation, IEEE Trans. Med. Imag. 37 (2) (Feb 2018).

[10] Jingxu Xua, Depeng Xua, Qianyue Weib, Yongjin Zhoua, Automatic Classification of Male and Female Skeletal Muscles Using Ultrasound Imaging, Biomedical Signal Processing and Control, Elsevier, Oct 2019.

[11] Reza Rasti, Hossein Rabbani, Alireza Mehridehnavi, Fedra Hajizadeh, Macular OCT classification using a multi-ScaleConvolutional neural network ensemble, IEEE Trans. Med. Imag. 37 (4) (April 2018).

[12] Guilherme F. Roberto, Marcelo Z. Nascimento, Alessandro S. Martins, Thaína A. .A. Tosta, Paulo R. Faria, Leandro A. Neves, "Classification of Breast and Colorectal Tumors Based on Percolation of Color Normalized Images", Computers & Graphics, Elsevier, Sep 2019.

[13] Rui Yan, Fei Ren, Zihao Wang, Lihua Wang, Tong Zhang, Yudong Liu, Xiaosong Rao, Chunhou Zheng, Fa Zhang, "Breast Cancer Histopathological Image Classification Using a Hybrid Deepneural Network", Methods, Elsevier, Jul 2019.

[14] ChristopherSyben Andreas Maier, TobiasLasser, ChristianRiess, A Gentle Introduction to Deep Learning in Medical Image Processing", Elsevier, Dec 2018. Review.

[15] A.S. Lundervold, A. Lundervold, An overview of deep learning in medical imaging focusing on MRI, Zeitschrift für Medizinische Physik 29 (2) (May 2019) 102–127.

[16] Shuchao Pang, Anan Du, Mehmet A. Orgun, Zhezhou Yu, A Novel Fused Convolutional Neural Network for Biomedical Image Classification, Springer, Jul 2018. Medical & Biological Engineering & Computing.

[17] Dongyun Lin, Lei Sun, Kar-Ann Toh, Jing Bo Zhang, Zhiping Lin, Biomedical image classification based on a cascade of an SVM with a reject option and subspace analysis. Computers in Biology and Medicine, Elsevier, Mar 2018.

[18] Chi-Chang Clayton Chen, Jyh-Wen Chai, Hung-Chieh Chen, Hsin Che Wang, Yung-Chieh Chang, Yi-Ying Wu, Wen-Hsien Chen, Hsian-Min Chen, San-Kan Lee, Chein-I Chang, An Iterative Mixed Pixel Classification for Brain Tissues and White Matter Hyperintensity in Magnetic Resonance Imaging", IEEE Access, Jul 2019.

[19] Yun Gu, Mali Shen, Jie Yang, Guang-Zhong Yang, Reliable Label-Efficient Learning for Biomedical Image Recognition, IEEE Transactions on Biomedical Engineering, Mar 2018.

[20] Philipp Seebock, Sebastian M. Waldstein, Sophie Klimscha, Hrvoje Bogunovic, Thomas Schlegl, Bianca S. Gerendas, René Donner, Ursula Schmidt-Erfurth, Georg Langs, Unsupervised Identification of Disease Marker Candidates in Retinal OCT Imaging Data, IEEE Transactions on Medical Imaging, Apr 2019.